



## Communication

## Mixed valence as a necessary criteria for quasi-two dimensional electron gas in oxide hetero-interfaces

Vijeta Singh<sup>a,b,\*</sup>, J.J. Pulikkotil<sup>a,b</sup><sup>a</sup> Academy of Scientific & Innovative Research (AcSIR), CSIR-National Physical Laboratory, New Delhi 110012, India<sup>b</sup> Council of Scientific and Industrial Research, National Physical Laboratory, New Delhi 110012, India

## A B S T R A C T

The origin of quasi-two dimensional electron gas at the interface of polar-nonpolar oxide hetero-structure, such as  $\text{LaAlO}_3/\text{SrTiO}_3$ , is debated over electronic reconstruction and defects/disorder models. Common to these models is the partial valence transformation of substrate Ti ions from its equilibrium  $4+$  state to an itinerant  $3+$  state. Given that the Hf ions have a lower ionization potential than Ti due to the  $4f$  orbital screening, one would expect a hetero-interface conductivity in the polar-nonpolar  $\text{LaAlO}_3/\text{SrHfO}_3$  system as well. However, our first principles calculations show the converse. Unlike the  $\text{Ti}^{3+} - \text{Ti}^{4+}$  valence transition which occur at a nominal energy cost, the barrier energy associated with its isoelectronic  $\text{Hf}^{3+} - \text{Hf}^{4+}$  counterpart is very high, hence suppressing the formation of quasi-two dimensional electron gas at  $\text{LaAlO}_3/\text{SrHfO}_3$  hetero-interface. These calculations, therefore, emphasize on the propensity of mixed valence at the interface as a necessary condition for an oxide hetero-structure to exhibit quasi two-dimensional electron gas.

The origin of quasi-two dimensional electron gas at the interface of  $\text{LaAlO}_3/\text{SrTiO}_3$  [1] and few other perovskite hetero-structures and super-lattices has been attributed to both intrinsic and extrinsic factors [2–5]. Among these, the most fascinating and widely discussed model is that of electronic reconstruction due to polar catastrophe. According to the model, a polar discontinuity emerges due to the polar ( $\text{LaAlO}_3$ ) and non-polar ( $\text{TiO}_2$  terminated  $\text{SrTiO}_3$ ) interface [6,7], leading to a potential build-up which concomitantly increase with increasing  $\text{LaAlO}_3$  film thickness. In case of an abrupt interface, i.e., devoid of defects and disorder, electronic stability at the interface is accomplished by a charge transfer from the  $\text{LaAlO}_3$  surface to the interface  $\text{TiO}_2$  layer of the  $\text{SrTiO}_3$  substrate, thereby leading to a superposition of  $\text{Ti}^{4+}$  and  $\text{Ti}^{3+}$  states at the interface. The extra electron in the  $3d$  band of  $\text{Ti}^{3+}$  render the hetero-interface conductivity. The picture is well justified in terms of spectroscopy and band structure calculations [8–10]. With increasing film thickness, the valence  $O\ 2p$  bands emanating from the  $\text{LaAlO}_3$  surface move towards the Fermi energy until it overlaps with the  $\text{SrTiO}_3$  conduction band. The orbital overlap occurs at a certain critical thickness of the  $\text{LaAlO}_3$  film, below which the polar discontinuity appears to be alleviated by field induced polar distortions in the near-interface layers of  $\text{SrTiO}_3$  [11–13].

Simplest among the alternate mechanisms to the polar catastrophe model that lead to quasi-two dimensional conductivity at the interface of oxide heterostructures is the defect/disorder models [14–18]. Following the growth process, such as the pulsed laser deposition

technique, it may be well assumed that this high energy synthesis would facilitate  $\text{La}^{3+}/\text{Sr}^{2+}$  and/or  $\text{Al}^{3+}/\text{Ti}^{4+}$  inter-mixing at the interface thereby reducing the extent of polar catastrophe at the interface [7,19]. Beyond, defects in the form of oxygen vacancies, the concentration of which depends sensitively on the growth parameters, also tend to modify the interface structure and electronic properties [22–25]. For example, an oxygen vacancy holds its equivalence to two extrinsically doped electrons into the system which could also alleviate the polar discontinuity at the interface. Thus, based on simple valence arguments, defects in the form of oxygen vacancies and/or inter-site cation disorder would also induce electronic conductivity via the superposition of  $\text{Ti}^{3+}$  and  $\text{Ti}^{4+}$  states at the interface. Apart from these extrinsic effects, it is also proposed that lattice instabilities could also drive the  $\text{LaAlO}_3/\text{SrTiO}_3$  interface conducting [28]. In general, both intrinsic (polar discontinuity) and extrinsic (defects and disorder) mechanisms are expected to play an important role in driving the hetero-interface towards instability.

Thus, irrespective of the above models, the origin of quasi-two dimensional electron gas (q-2DEG) in oxide hetero-structures, seem to be a facilitation of mixed valence states of the Ti transition metal at the interface [26,27]. Moreover, the relative stability of the  $\text{Ti}^{3+}$  valence state is fairly high, as is being evidenced by phase diagrams, where  $\text{SrTiO}_3$  form a continuous solid solutions with electron doping (the case of La substitutions at the Sr site). Beyond, the high structural stability of  $\text{SrTiO}_3$  withstanding oxygen vacancies as high as 10% and also the

\* Corresponding author at: Academy of Scientific &amp; Innovative Research (AcSIR), CSIR-National Physical Laboratory, New Delhi 110012, India.

large oxygen ionic mobility in  $\text{SrTiO}_3$  could be well associated to the intrinsic chemical property of the Ti ions via valence regulation between its energetically favorable  $3+$  and  $4+$  states. Along these perspectives, it then becomes rudimentary to check for the necessary and sufficient conditions in oxide hetero-interface conductivity, directed towards the role of multiple valence states of the substrate.

The propensity of an ion to exhibit multiple valence states in group IV B of the periodic table decrease down the group. In this regard, we consider the  $\text{LaAlO}_3/\text{SrXO}_3$  oxide hetero-structures with  $\text{XO}_2$  termination of the substrate,  $\text{X} \equiv \text{Ti}$  and  $\text{Hf}$ . In this isoelectronic class of systems, the stability of Ti in its  $+3$  and  $+4$  states in  $\text{SrTiO}_3$  are ubiquitous [20,21], while the propensity of Hf exhibiting multiple valence states is little known. It is also worthy to mention that  $\text{SrTiO}_3$  accommodate chemical substitutions at both Sr and Ti sites forming a complete solid solutions, while such cases tend to be very limited for  $\text{SrHfO}_3$ . Hence, based on these observations and, considering that the electronic conductivity in oxide hetero-structures proportionate with the concentration of interface mixed valence states, one would then expect a steady decline in the transport properties as the transition metal in  $\text{SrXO}_3$  substrate is replaced from Ti to Hf. On the other hand, comparison of the ionization energies of Ti ( $\approx 6.8$  eV) and Hf ( $\approx 5.9$  eV) shows that the latter have lower ionization energy due to the lanthanide contraction, where the  $4f$  electrons screen the positive nuclear charge from the outer  $5d$  valence electrons. In this pretext, one may then expect a q-2DEG at the hetero-interface of  $\text{LaAlO}_3/\text{SrHfO}_3$ , similar to that of its isoelectronic  $\text{LaAlO}_3/\text{SrTiO}_3$  counterpart, which would then reveal a rare instance of Hf ions in the non-equilibrium  $+3$  state.

To illustrate that the necessary condition to impart a q-2DEG at an abrupt hetero-interface is electronic reconstruction of the transition metal ions, we adopt to the first-principles calculations based on density functional theory (DFT). The DFT approach to the problem has remained quite successful in illustrating the hetero-interface conductivity of  $\text{LaAlO}_3/\text{SrTiO}_3$ . The calculations were carried out using the full-potential linearized augmented plane-wave (FP-LAPW) method, as implemented in the WIEN2k suite of programs [29]. The hetero-structures were modeled by stacking five unit cells of  $\text{SrXO}_3$  with  $\text{XO}_2$  termination ( $\text{X} \equiv \text{Ti}$ ,  $\text{Hf}$ ) as substrate while the  $\text{LaAlO}_3$  film was assigned four unit-cells thickness. The structural dimension of the hetero-structure was  $\sqrt{2}a \times \sqrt{2}a \times c$ , with  $a=3.905$  and  $4.117$  Å for the  $\text{LaAlO}_3/\text{SrTiO}_3$  and  $\text{LaAlO}_3/\text{SrHfO}_3$  substrates, respectively and  $c=9a$ . The periodic images of the system is further separated by a vacuum separation of  $55$  Å. This geometry provides an extra degree of freedom to the surface ions to relax outwards while equilibrating the internal ionic coordinates with minimum forces between the ions. The exchange-correlation potential was described in the generalized gradient approximation (GGA). Convergence in the basis set was achieved with  $\text{RK}_{\text{max}} = 7$ , R being the smallest LAPW sphere radius and  $\text{K}_{\text{max}}$  being the interstitial plane-wave cutoff. The sphere radii, in Bohr units, for Sr/La, Ti/Hf, and O were chosen as 2.2, 1.9, and 1.6, respectively. Convergence of the Brillouin zone (BZ) sampling is achieved for a Monkhorst-Pack  $k$ -mesh of dimension  $15 \times 15 \times 2$ , equivalent to 72  $k$ -points in the irreducible region of the BZ.

In Fig. 1 we show the band structure of  $\text{LaAlO}_3/\text{SrTiO}_3$  and  $\text{LaAlO}_3/\text{SrHfO}_3$  hetero-structures. The conduction bands of  $\text{LaAlO}_3/\text{SrHfO}_3$  are comprised of the Ti  $3d$  states of the  $\text{SrTiO}_3$  substrate, while the valence band is predominantly O  $2p$  in character. However, the interesting feature that merges from the site-decomposed orbital projection of the band structure shows that the bottom of the valence band ( $E - E_F < 2$  eV, not shown) is mainly composed of the O  $2p$  bands emanating from the  $\text{SrTiO}_3$  substrate, while the top ( $-2$  eV  $< E < E_F$ ) is predominantly of those emanating from the  $\text{AlO}_2$  layers of the  $\text{LaAlO}_3$  motif. The weight factor in the distribution of the  $\text{AlO}_2$  derived O  $2p$  states, however, increase in energy as one moves from the interface towards the surface. The bands that cross the Fermi energy are those of the O  $2p$  states of the surface  $\text{AlO}_2$  layer. Similarly, we also find a layer by layer distribution of Ti  $3d$  energy states in the conduction band. We

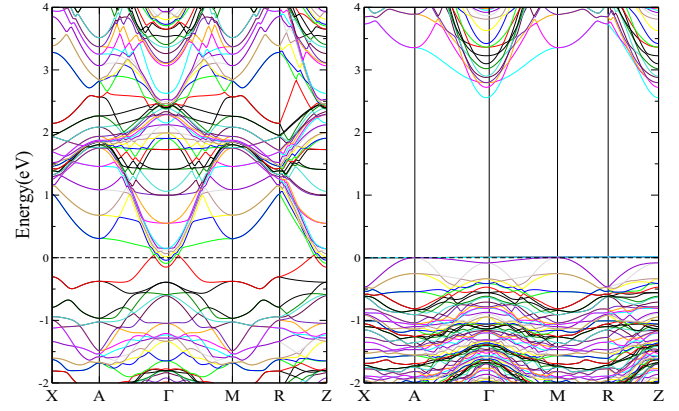


**Fig. 1.** (Color Online) The band structure of  $\text{LaAlO}_3 - \text{SrTiO}_3$  (left panel) and  $\text{LaAlO}_3 - \text{SrHfO}_3$  (right panel). The horizontal line through energy zero represents the reference Fermi energy.

note that the Ti  $3d$  states of bulk  $\text{SrTiO}_3$  are  $> 3.2$  eV ( $\equiv E_g$ ; the band gap) are above the valence band maximum. However, as one moves towards the interface, the energy of Ti  $3d$  bands are lowered in energy, in a layer-by-layer fashion and one observes that the  $3d$  bands emanating from the interface Ti ions cross the Fermi energy. Thus, the Fermi energy is composed of surface O  $2p$  bands as well as interface Ti  $3d$  bands. This is consistent with the predictions of the polar catastrophe model, suggesting an electronic reconstruction of the interface Ti bands via transfer of electrons from the  $\text{LaAlO}_3$  film.

In case of  $\text{LaAlO}_3/\text{SrHfO}_3$  hetero-structures, we find no band crossing at the Fermi energy. The ground state is insulating with an electronic band gap of 2.6 eV. It may be noted that the estimated band gap from the calculations may be significantly underestimated, in the light of the knowledge that the experimentally measured  $\text{SrTiO}_3$  band gap of 3.2 eV is  $\approx 40\%$  smaller (1.9 eV) in the GGA calculations. Similarly, the calculated GGA band gap of bulk  $\text{SrHfO}_3$  in its cubic perovskite structure is determined to be 3.8 eV against the experimental value of 6.1 eV [30], i.e.,  $\approx 37\%$  underestimation with regard to experimental value. However, the exact value of the electronic band gap seems to be of little relevance in the present context. Irrespective of the band gap underestimation, first-principles calculations employing both local density approximation (LDA) or GGA consistently reproduce the critical thickness of 4 unit-cells of  $\text{LaAlO}_3$  to impart conductivity at the  $\text{LaAlO}_3/\text{SrHfO}_3$  hetero-interface [11,31,32]. In Fig. 2, we show the partial density of states (PDOS) of the Hf and Ti sub-lattice of the 4 unit-cell thick  $\text{LaAlO}_3/\text{SrHfO}_3$  and  $\text{LaAlO}_3/\text{SrTiO}_3$  systems, respectively. The overall features are in good agreement with those reported in Ref.

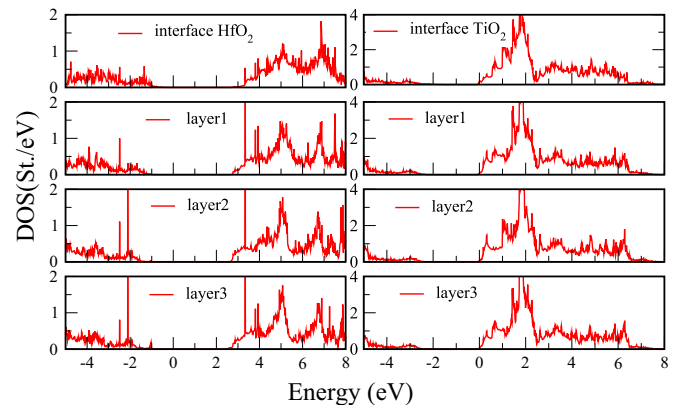


**Fig. 2.** (Color Online) PDOS of  $\text{LaAlO}_3 - \text{SrHfO}_3$  (left panel) and  $\text{LaAlO}_3 - \text{SrTiO}_3$  (right panel). It shows layer resolved DOS calculated using GGA. The zero on the energy scale represent the  $E_F$ .

[21]. As evident, from the figure, the interface Ti 3d states cross the  $E_F$ , while in  $\text{LaAlO}_3/\text{SrHfO}_3$  no finite states are observed at  $E_F$ .

Beyond, a comparison of the  $\text{LaAlO}_3/\text{SrHfO}_3$  and  $\text{LaAlO}_3/\text{SrTiO}_3$  band structures show that there is a rigid band like shift of the transition metals  $d$ - states in the conduction band. However, such a case is not true for the O 2p bands that constitute the upper valence band. They are at variance in both dispersion as well as in position from the Fermi energy. While in  $\text{LaAlO}_3/\text{SrHfO}_3$ , the surface  $\text{AlO}_2$  emanating O 2p are more dispersed over the energy range of  $-0.5$  to  $+0.1$  eV ( $E=0$  referring to the reference Fermi energy,  $E_F$ ), they appear to much narrower in  $\text{LaAlO}_3/\text{SrHfO}_3$  with a dispersion range between  $-0.1$  eV to  $E_F$ . This unequivocally suggests that the energy scales associated with valence band alignment of  $\text{LaAlO}_3$  to that of the substrate  $\text{SrXO}_3$  conduction bands are very different, although the interface of both  $\text{LaAlO}_3/\text{SrHfO}_3$  and  $\text{LaAlO}_3/\text{SrTiO}_3$  hetero-structures develop similar polar-discontinuity.

Despite having a polar discontinuity at the interface of  $\text{LaAlO}_3/\text{SrHfO}_3$  hetero-structure, the question is “what then relaxes the polar instability developed at the hetero-interface of  $\text{LaAlO}_3/\text{SrHfO}_3$ ” To address, we seek explanation within the realms of parallel plate capacitor model. For two infinitely extended oppositely charged plates separated by distance  $d$ , which here represents the inter-planar ( $\text{LaO})^+$  and  $(\text{AlO})^-$  distance, the potential  $V \propto d$ , assuming that both charge and the dielectric constant remains unchanged. In this backdrop, it is also important to note that a change in dielectric constant is possible in these systems due to lattice strain. In comparison to the  $\text{LaAlO}_3/\text{SrHfO}_3$  which has a lattice mismatch of  $\approx 3\%$ , for  $\text{LaAlO}_3/\text{SrTiO}_3$  this amounts to  $\approx 8\%$ , evidencing large strain at the hetero-interface. Beyond, it is generally found that compressive strain decreases the dielectric constant in the perovskite structure, while the tensile strain enhances the dielectric constant in a parallel plate capacitor [33–35]. We also note that system with much larger interface strain have been synthesized and characterized. For example, a comparison of the lattice constant of  $\text{SrZrO}_3$  and  $\text{SrTiO}_3$  mounts to a 6% mismatch, however, have been successfully grown by various groups.

To investigate whether structural distortion and/or atomic relaxation play any role in alleviating the polar catastrophe at the hetero-interface, we carry out the structure optimization for the hetero-structures by using force optimization using the scalar-relativistic Hamiltonian. In these, we discover interesting features relevant to the present discussion. In Fig. 3 we show the change in the cationic inter-planar distance of both  $\text{LaAlO}_3/\text{SrTiO}_3$  and  $\text{LaAlO}_3/\text{SrHfO}_3$

hetero-structures. What follows from Fig. 3 is a systematic variation in the negatively ( $\text{Al}^{3+}\text{O}_2^{2-}$ ) and positively ( $\text{La}^{3+}\text{O}^{2-}$ ) charged inter-planar distances along the crystallographic  $c$ -axis, as one move from the surface  $\text{LaAlO}_3$  to the  $\text{SrXO}_3$  substrate. We find that the Al-Al  $c$ -axial ionic distance is compressed significantly in  $\text{LaAlO}_3/\text{SrHfO}_3$ , far more higher in comparison with its isoelectronic  $\text{LaAlO}_3/\text{SrTiO}_3$  system. For instance, the Al-Al  $c$ -axial bond distance near to the surface is twice larger compressed in  $\text{LaAlO}_3/\text{SrHfO}_3$  than  $\text{LaAlO}_3/\text{SrTiO}_3$ . However, as one approaches the  $\text{LaO} - \text{TiO}_2$  hetero-interface from the surface, the distance between the  $\text{AlO}_2$  planes decrease, converging to their equilibrium value.

Similarly, marked deviation in the inter-ionic  $c$ -axial distances are also observed between the La-La ions which constitute the film overlayers. The relaxation of the  $\text{TiO}_2$  ( $\text{HfO}_2$ ) planes in the respective  $\text{SrTiO}_3$  ( $\text{SrHfO}_3$ ), however, appears to be less altered owing to their charge. Thus, it follows that maximum bonding modulations are observed at the two interfaces, i.e., (i) at the hetero-interface of non-polar  $\text{TiO}_2$  with polar  $\text{LaO}$  layer and, (ii) that at the polar  $\text{AlO}_2$  layer of the  $\text{LaAlO}_3$  film surface with vacuum. The maximum compression is, however, observed in the proximity of the negatively charged  $\text{AlO}_2$  – vacuum interface. Although small, the change in the X-X bond distances of the substrate along the  $c$ -axis, in the hetero-interfacial region are also of certain importance. Considering the atomic-mass of Hf, a displacement of such massive ions from its equilibrium position amounts to higher energy, the source of which is derived from the energy associated with the built-in interface polar discontinuity.

Thus, we find at least two intrinsic mechanisms that prevail in such oxide hetero-structures, which compete accordingly to the nature of the ions that represent the hetero-interface. Since, the Ti ions in  $\text{TiO}_2$  terminated  $\text{SrTiO}_3$  have a greater propensity to form multi-valent states, the potential build-up due to polar discontinuity in  $\text{LaAlO}_3/\text{SrTiO}_3$  hetero-structure is partly alleviated by means of both atomic relaxation as well as electronic reconstruction. The electronic reconstruction facilitates conductivity at the hetero-interface in the form of a quasi- two dimensional electron gas. Along these perspectives, the absence of hetero-interface conductivity in  $\text{LaAlO}_3/\text{SrHfO}_3$  reflects to the impedance of  $\text{Hf}^{4+} \rightarrow \text{Hf}^{3+}$  chemical reduction, although the ionization potential of Hf ion is smaller than that of Ti. The impedance of  $\text{Hf}^{3+}$  in the interfacial  $\text{HfO}_2$  layers of the  $\text{SrHfO}_3$  substrate appears to be associated with steric interactions. As per empirical calculations, the ionic radius of  $\text{Hf}^{4+}$  (91 pm) upon reduction to  $\text{Hf}^{3+}$  increases to 103 pm, which may not fit into the lattice [36]. Thus, with the in-plane lattice parameter being constrained to that of the substrate, the polar catastrophe which mounts with  $\text{LaAlO}_3$  film thickness is alleviated along the  $c$ - axis, with decreasing inter-planar distance towards the surface from the hetero-interface. Such a relaxation abide by the parallel plate capacitor model characteristics. The flow of charge from the  $\text{AlO}_2$  surface could be impeded by decreasing the distance between the negatively charged  $\text{AlO}_2$  and positively charge  $\text{LaO}$  plates, according to the basic relation  $V \propto d$ . Consequently, as the distance between the charged plates are decreased, the potential build-up at the hetero-interface would also decrease. These results, derived out of our first-principles calculations point to a direction of experimental validation so as to ascertain (i) the importance of multi-valent ions at the hetero-interfaces for 2DEG, (ii) relevance of structural relaxation (and/or atomic reconstruction) at both hetero-interface and at hetero-surface.

To summarize, the interface properties of polar-nonpolar  $\text{LaAlO}_3/\text{SrTiO}_3$  and  $\text{LaAlO}_3/\text{SrHfO}_3$  hetero-structures are studied within the realms of DFT methods. With 4f electrons of Hf ions partly screening the valence charge, the ionization potential of Hf ions is significantly lowered and thus expected that the polarity driven interface potential would drive in a quasi-two dimensional electron gas at the hetero-interface of  $\text{LaAlO}_3/\text{SrHfO}_3$ , similar to its isoelectronic  $\text{LaAlO}_3/\text{SrTiO}_3$  counterpart. However, formation of non-equilibrium  $\text{Hf}^{3+}$  states are forbidden in the  $\text{LaAlO}_3/\text{SrHfO}_3$ , rendering the interface insulating. The electrostatic potential build-up at the interface is, in turn, nullified

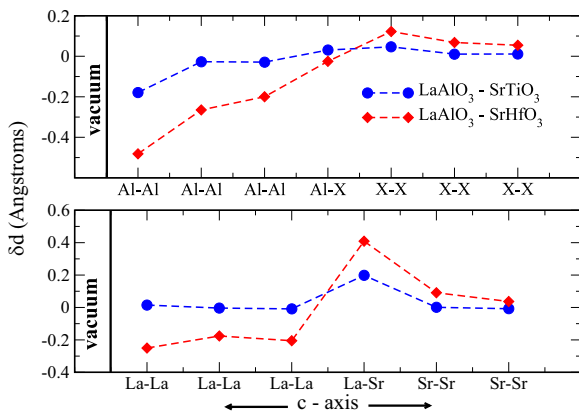


**Fig. 3.** The deviation in the inter-ionic distances between the negatively charged  $(\text{AlO}_2)^-$  planes, positively charged  $(\text{LaO})^+$  planes and charge neutral  $\text{XO}_2$  ( $\text{X}=\text{Ti}$  and  $\text{Hf}$ ) and  $\text{SrO}$  planes along the crystallographic  $c$ -axis in  $\text{LaAlO}_3 - \text{SrTiO}_3$  and  $\text{LaAlO}_3 - \text{SrHfO}_3$  hetero-structures, from the fully relaxed force optimized structure, in comparison to the their bulk cubic perovskite value (3.905 Å for  $\text{SrTiO}_3$  and 4.117 for  $\text{SrHfO}_3$ ). The X-X ionic distances in the upper panel refer to the Ti-Ti and Hf-Hf bond distances of the respective hetero-structure. The dashed lines serve as a guide to the eye.

by inter-planar ionic relaxation. Calculations reveal that the inter-planar distance between the charged  $(\text{AlO}_2)^-$  and  $(\text{LaO})^+$  planes of the  $\text{LaAlO}_3/\text{SrHfO}_3$  hetero-structure are renormalized, with the planes near the surface being significantly compressed. This is in tandem with the parallel plate capacitor model, where the electrostatic potential proportionate with inter-planar distance ( $V \propto d$ ). A decrease in  $d$  therefore reduces the extent of polar catastrophe at the interface. Thus, our calculations infer that the polar catastrophe may be necessary criteria for an oxide hetero-interface to display quasi-2DEG, however, is not sufficient. Nevertheless, it is the propensity of transition metal ions to exhibit multi-valent states, the most necessary criteria and in cases where inter-valence transition is suppressed, the electrostatic instability due to polar discontinuity is compensated by means of structural modulations.

## Acknowledgments

JJP acknowledges funding from Department of Science and Technology (DST, Project# EMR/2014/0001004) Government of India. VS thanks CSIR for a senior research fellowship.

## References

- [1] A. Ohtomo, H.Y. Hwang, *Nature* 427 (2004) 423–426.
- [2] D.S.J. Mannhart, *Science* 327 (2010) 1607–1611.
- [3] P. Zubko, S. Gariglio, M. Gabay, P. Ghosez, J.-M. Triscone, *Annu. Rev. Condens. Matter Phys.* 2 (2011) 141.
- [4] S.A. Pauli, P.R. Willmott, *J. Phys.: Condens. Matter* 20 (2008) 264012.
- [5] C. Li, Q. Xu, Z. Wen, S. Zhang, A. Li, D. Wu, *Appl. Phys. Lett.* 103 (2013) 201602.
- [6] N. Nakagawa, H.Y. Hwang, D.A. Muller, *Nat. Mater.* 5 (2006) 204.
- [7] L. Qiao, T.C. Droubay, T.C. Kaspar, P.V. Sushko, S.A. Chambers, *Surf. Sci.* 605 (2011) 1381.
- [8] J.-S. Lee, Y.W. Xie, H.K. Sato, C. Bell, Y. Hikita, H.Y. Hwang, C.-C. Kao, *Nat. Mater.* 12 (2013) 703.
- [9] A. Rastogi, J.J. Pulikkotil, S. Auluck, Z. Hossain, R.C. Budhani, *Phys. Rev. B* 86 (2012) 075127.
- [10] R. Claessen, M. Sing, M. Paul, G. Berner, A. Wetscherek, A. Müller, W. Drube, *New J. Phys.* 11 (2009) 125007.
- [11] R. Pentcheva, W. Pickett, *Phys. Rev. Lett.* 102 (2009) 107602.
- [12] G. Singh-Bhalla, C. Bell, J. Ravichandran, W. Siemons, Y. Hikita, S. Salahuddin, A.F. Hebard, H.Y. Hwang, R. Ramesh, *Nat. Phys.* 7 (2011) 80.
- [13] Z.S. Popović, S. Satpathy, R.M. Martin, *Phys. Rev. Lett.* 101 (2008) 256801.
- [14] P. Kumar, A. Dogra, V. Toutam, *Appl. Phys. Lett.* 103 (2013) 211601.
- [15] T. Ohnishi, K. Shibuya, T. Yamamoto, M. Lippma, *J. Appl. Phys.* 103 (2008) 103703.
- [16] C.W. Schneider, M. Esposito, I. Marozau, K. Conder, M. Doebeli, Yi Hu, M. Mallepell, A. Wokaun, T. Lippert, *Appl. Phys. Lett.* 97 (2010) 192107.
- [17] J.J. Pulikkotil, S. Auluck, P. Kumar, A. Dogra, R.C. Budhani, *Appl. Phys. Lett.* 99 (2011) 081915.
- [18] Z.Q. Liu, W. Lu, S.W. Zeng, J.W. Deng, Z. Huang, C.J. Li, M. Motapothula, W.M. Lü, L. Sun, K. Han, J.Q. Zhong, P. Yang, N.N. Bao, W. Chen, J.S. Chen, Y.P. Feng, J. M.D. Coey, T. Venkatesan and Ariando, *Advance Materials Interfaces*, 1400155, 2014.
- [19] S.A. Chambers, M.H. Engelhard, V. Shutthanandan, Z. Zhua, T.C. Droubay, L. Qiao, P.V. Sushko, T. Feng, H.D. Lee, T. Gustafsson, E. Garfunkel, A.B. Shah, J.-M. Zuo, Q.M. Ramasse, *Surface Science Reports*, 65, 31, 7, 2010.
- [20] A. Sorokine, D. Bocharov, S. Piskunov, V. Kashcheyevs, *Phys. Rev. B* 86 (15) (2012) 155410.
- [21] J. Verbeeck, S. Bals, A.N. Kravtsova, D. Lamoen, M. Luysberg, M. Huijben, G. Rijnders, A. Brinkman, H. Hilgenkamp, D.H.A. Blank, G. Van Tendeloo, *Phys. Rev. B* 81 (8) (2010) 085113.
- [22] W. Siemons, G. Koster, H. Yamamoto, W.A. Harrison, G. Lucovsky, T.H. Geballe, D.H.A. Blank, M.R. Beasley, *Phys. Rev. Lett.* 98 (2007) 196802.
- [23] C. Cancellieri, N. Reyren, S. Gariglio, A.D. Caviglia, A. Fête, J.-M. Triscone, *Europhys. Lett.* 91 (2010) 17004.
- [24] A. Brinkman, M. Huijben, M. van Zalk, J. Huijben, U. Zeitler, J.C. Maan, W.G. van der Wiel, G. Rijnders, D.H.A. Blank, H. Hilgenkamp, *Nat. Mater.* 6 (2007) 493.
- [25] N.J. Eckstein, *Nat. Mater.* 6 (2007) 473.
- [26] S. Thiel, G. Hammerl, A. Schmehl, C.W. Schneider, J. Mannhart, *Science* 313 (2006) 1942.
- [27] K. Yoshimatsu, R. Yasuhara, H. Kumigashira, M. Oshima, *Phys. Rev. Lett.* 101 (2008) 026802.
- [28] P.W. Lee, V.N. Singh, G.Y. Guo, H.J. Liu, J.C. Lin, Y.H. Chu, C.H. Chen, M.W. Chu, *Nat. Commun.* 7 (2016) 12773.
- [29] P. Blaha, K. Schwarz, G. Madsen, D. Kvasika, J. Luitz, *Computer code WIEN2K*, Technial University of Vienna, 2001.
- [30] C. Rossel, M. Sousa, C. Marchiori, J. Fompeyrine, D. Webb, D. Caimi, B. Mereu, A. Ispas, J.P. Locquet, H. Siegwart, R. Germann, A. Tapponnier, K. Babich, *Microelectron. Eng.* 84 (2007) 1869.
- [31] S. Ishibashi, K. Terakura, *J. Phys. Soc. Jpn.* 77 (2008) 104706.
- [32] H. Chen, A.M. Kolpak, S. Ismail-Beigi, *Phys. Rev. B* 79 (2009) R161402.
- [33] T. Shimizu, *Solid State Commun.* 102 (1997) 523.
- [34] T.M. Shaw, Z. Suo, M. Huang, E. Liniger, R.B. Laibowitz, J.D. Baniecki, *Appl. Phys. Lett.* 75 (1999) 2129.
- [35] S. Hyun, K. Char, *Appl. Phys. Lett.* 79 (2001) 254.
- [36] D. Eder, R. Kramer, *Phys. Chem. Chem. Phys.* 4 (2002) 795.